

Influence of NaOH concentration on the decolorization of crystal violet dyed cotton fabric

Kristen Mardenborough¹, Maya Florentino¹, Robert Haxhari¹, Yu-Chung Lin¹, Miriam Rafailovich¹, Gary Halada¹, Hye Jung Jung^{2†*}, Taejin Kim1[†]*

¹School 1 Department of Materials Science and Chemical Engineering, Stony Brook University, Stony Brook, New York 11794, United States ²DaVinci College of General Education, Chung-Ang University, Seoul, South Korea *These authors contributed equally to this work

Received December 28, 2021 Revised March 12, 2022 Accepted April 17, 2022

ABSTRACT

Synthetic dye removal is a topic of increasing interest as textile recycling has become more popular in industries. While methods involving dye removal from wastewater effluent have been widely studied and reported on, research on decolorization of fabric itself remains quite unknown. In regard to the lack of research, this study presents cotton fabric samples dyed with crystal violet (CV) that were treated with varying concentrations of sodium hydroxide (NaOH). Fabric decolorization was studied using several characterization methods. Scanning electron microscopy (SEM), Fourier transform infrared spectroscopy (FTIR), and Raman spectroscopy data showed that the cellulose structure remained unchanged after CV and NaOH treatment. Characteristic CV peaks in the FTIR and Raman spectra were apparent only in the control sample, while the spectra of NaOH-treated samples were very similar to that of the cotton fabric. X-ray diffractometry (XRD) data also confirmed that the crystallite size of cellulose was not affected by CV and NaOH treatment. A visible violet hue remained in all NaOH-treated samples, though CV intensity was inversely proportional to NaOH concentration. The L*a*b* values were utilized to complement characterization results. As the concentration of NaOH was increased, the CIELAB parameters aligned more with those of the plain untreated fabric

Keywords: Cotton fabric, crystal violet, decolorization, L*a*b*, microscopy, spectroscopy

1. Introduction

End-of-life waste management has become an increasingly urgent issue that has prompted research into how transitioning from a linear to a circular textile economy can prolong product life and decrease solid waste in landfills [1, 2]. In the United States, textiles accounted for 5.8 % of total municipal solid waste in 2018, with only 14.7 % of this waste being recycled according to the Environmental Protection Agency (EPA) [3]. In 2015, the growth of cotton and production of finished textiles required 98 billion kilograms of non-renewable resources such as oil, chemicals, and fertilizers [4]. Textile recycling has become attractive to prevent its accumulation in landfills, limit the usage of nonrenewable resources, and lessen the environmental damage caused by its manufacturing. For recycling waste cotton, the development of recycling practices that can be used regardless of variability in the post-consumer products, fiber aging, and the production of high-quality products from recycled cotton that are marketable must be addressed [5].

Research into textile dye removal from cotton has aimed to extend the product life cycle while retaining the structural integrity of the material [2, 6]. Using ozonation, sonolysis, Fenton's processes, biodegradation, and base chemicals, dye removal and degradation from wastewater and textiles has been achieved, though each method has advantages and disadvantages [7-10] For instance, sonolysis results in decolorization of dyed textiles, but the kinetics are very slow if not coupled with other techniques (i.e., hydrogen peroxide, ozone, and Fenton). Fenton's photo-



This is an Open Access article distributed under the terms of the Creative Commons Attackers 27 of the Creative Commons Attribution Non-Commercial License (http://creativecommons.org/licenses/by-nc/3.0/) which per-

mits unrestricted non-commercial use, distribution, and reproduction in any medium, provided the original work is properly cited.

Copyright © 2023 Korean Society of Environmental Engineers

† Corresponding author

E-mail: (H.J.J.) jayjung@cau.ac.kr, (T.K.) taejin.kim@stonybrook.edu Tel: (H.J.J.) +82-10-8861-1980, (T.K.) +1-631-632-8433 Fax: (H.J.J.) +82-2-826-6029, (T.K.) +1-631-632-8052

ORCID: (H.J.J.) 0000-0002-4352-2816, (T.K.) 0000-0002-0096-303X

catalysis is feasible for the treatment of high concentration dve chemicals in textiles, however the reaction time is slow and requires low pH conditions (< 3.5) [11]. Biological processes have gained more attention due to their ecological benefit, however the high cost of enzymes, ability to control bacteria formation, creation of secondary pollutants, and low biodegradability of dye chemicals limits the value of these techniques [12, 13]. Base chemicals, including sodium hydroxide (NaOH), have been used to treat cotton fabric and cellulose [14-16]. This treatment method can also have added benefits such as low cost and simplicity of use. NaOH has been chosen in several studies as an effective, environmentally friendly chemical to enhance the dissolution of cellulose at higher concentrations [17-23]. Research, however, on the use of NaOH to specifically decolorize dyed cotton fabric has not been extensive. Therefore, using NaOH treatment for decolorization from textile is worthy to be investigated.

Crystal violet (CV), also known as gentian violet, is a triphenyl-methane synthetic dye that has many relevant uses, from dyeing and whitening fabric to its use as a topical treatment for fungal and bacterial infections [24, 25]. Azo dyes, such as CV, are commonly chosen as dyes for cotton textiles [26], leading to the selection of CV as a representative textile dye for this study. Studies have shown that CV solution can be decolorized using the hydroxide ion (OH) [27-29]. The conjugated double bonds in chromophores of CV give it specific color [16]. When CV reacts with NaOH, a dissociated hydroxide ion bonds to the central carbon, causing decolorization as the product is no longer conjugated.

In general, the reaction between CV and NaOH has only been studied extensively in aqueous solutions rather than in fabric. The novelty of this study is the elucidation of the reaction between CV and NaOH incorporated into solid material. After CV interacted with the cellulose in cotton fabric, different concentrations of NaOH were used to study the extent of decolorization. The results revealed that the decolorization of CV was dependent on the concentration of NaOH and that the molecular structure of cellulose remained unaffected after this reaction. To determine the molecular structure, morphology of the samples, and the extent of decolorization after the reaction, several characterization techniques were applied, including FTIR, Raman spectroscopy, XRD, SEM, and EDS. In addition to the characterization, mechanical strength and colorimetric analysis were also studied to understand the effect of CV and NaOH on the cotton fabric.

2. Experimental Section

2.1. Materials and Sample Preparation

Powdered crystal violet (CV, $C_{25}H_{30}N_3Cl$, ACS reagent, ≥ 90.0 %) and pellet form sodium hydroxide (NaOH, ACS reagent, ≥ 97.0 %) were purchased from Sigma-Aldrich and were utilized without pretreatment. Cotton fabric samples procured from Arthur R. Johnson Co., Inc., Brooklyn, N.Y. were provided by the Fashion Institute of Technology (FTT, U.S.A). Deionized water (~ 20 m Ω /cm, Direct-Q3, Millipore Sigma) was used to make 1.0×10^{-4} M CV stock solution and 0.1, 0.5, and 1.0 M NaOH stock solutions.

To prepare the CV-dyed cotton fabric samples, 1.5 cm \times 1.5 cm squares of cotton fabric were placed in separate beakers containing 10 mL of 1.0 \times 10⁻⁴ M CV solution. After ensuring that the pieces were fully submerged and covered by CV solution, the samples were left to soak overnight at room temperature. The CV-dyed samples were taken out of solution and placed into an oven overnight at \sim 60 °C. After removing the samples from the oven, 10 mL of the NaOH solutions were added to each dyed fabric sample. The fabric was kept in the NaOH solution overnight and removed the following day. The samples were placed in separate Petri dishes and again put in the oven to dry overnight at \sim 60 °C.

2.2. Characterization and Mechanical Testing

The infrared spectra were obtained with a Nicolet iS50 FTIR spectrometer (Thermo Fisher Scientific) equipped with an attenuated total reflectance (ATR) accessory. The samples were contacted with a diamond ATR crystal and the FTIR spectra (32 scans) were recorded between 400~4000 cm⁻¹ with a resolution of 4 cm⁻¹. Raman spectra were obtained using a Horiba-Jobin XploRATM PLUS Confocal Raman Microscope equipped with a 785 nm laser. Before collecting the Raman spectra of the sample, the spectrometer was calibrated via silicon material using a 100X objective and a 1200 gr/mm grating. The Raman spectra were collected in the 300~1800 cm⁻¹ and 2800~3300 cm⁻¹ Raman shift regions. The acquisition time was 10 seconds and then each spectrum was accumulated from 60 scans. Crystallite structures of the as-received and treated samples were examined using XRD. The XRD patterns were collected with a Philips PW1729/APD3520 diffractometer with copper radiation $(\lambda=1.54184 \text{ Å})$ in the 20 range of $20\sim80^{\circ}$ with a step size of 0.02 °. The surface topography and content were probed by SEM and EDS techniques, respectively. The SEM images were taken with LEO 1550 SFEG SEM (Zeiss) with an EDS detector from EDAX, and software/electronics from iXRFsystems. The samples were coated with nominally 6 nm of gold to reduce charging. Additionally, the samples were imaged using a Robinson backscatter detector (RBSD) and 20 keV electrons. Color measurements of the samples were performed using a ColorReader (Datacolor, U.S.A) and color values were compared by means of CIELAB parameters. The tensile strength, Young's modulus, and toughness of the woven cotton muslin samples were measured using an Instron 5542 testing station. The diameter of the cotton yarn sample was 250~300 μ m and the length of the sample was 150 mm. The extension rate was set at 2 mm/min.

3. Results and Discussion

3.1. Effect of NaOH Concentrations on CV Decolorization

To understand the decolorization of CV-dyed cotton fabric, digital photography and spectroscopic techniques, such as Fourier transform infrared and Raman spectroscopy, were applied. The cotton fabric as-received (Fig. 1(a)) had a yellow-like color. After the interaction between the positively charged CV (carbocation) and the negatively charged cotton fabric (OH-), the color changed from yellow to bluish-violet (Fig. 1(b)) [24, 28]. As shown in Fig. 1(c)-(e), the fading of the violet color increased with increasing

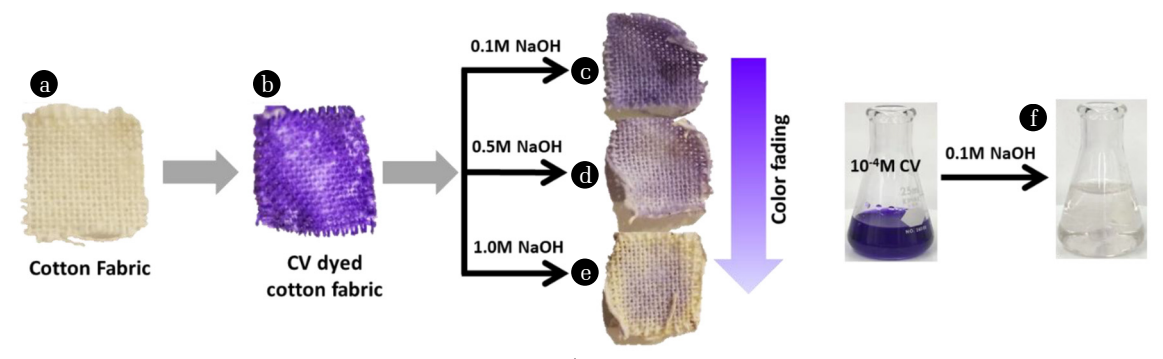


Fig. 1. Images of (a) cotton fabric (b) control (cotton fabric+1.0×10⁻⁴ M CV) sample (c) control sample treated by 0.1 M NaOH (d) control sample treated by 0.5 M NaOH (e) control sample treated by 1.0 M NaOH; ISO=800, 1/60 exposure time (f) 1.0 × 10⁻⁴ M M CV solution reaction with 0.1 M NaOH solution

NaOH concentration. The decolorization of CV in an alkaline (i.e., NaOH) aqueous media has been well documented. The rate of CV decolorization expressed as -r = k[CV][NaOH] where k is the rate constant [30]. Based on the rate equation, the CV decolorization reaction is first-order with respect to [NaOH]. It is worth noting that a bluish color was still evident in the NaOH-treated samples even at high NaOH concentrations (NaOH/CV = $1.0 \times 10^3 \sim 5.0 \times 10^3$). Because CV was fully decolorized in the liquid phase reaction under similar experimental conditions (Fig. 1(f)), it is expected that a cellulose-CV interaction decreases the decolorization rate, suggesting that the bond between cellulose and CV is stronger than the interaction between water and CV. This finding has two potential explanations. There may be an attractive force between the positively charged CV and negatively charged surface of the fabric causing adsorption [31]. When treated with NaOH, if attractive forces were predominantly present then it would be expected that the violet color of CV would be present in solution, which was not observed. Alternatively, there may be hydrogen bonding between cellulose and CV, supported by a probable overlapping of C-H and O-H peaks in the FTIR spectra of Fig. 2 [32].

3.2. Vibrational Spectroscopies

FTIR spectroscopy was utilized to examine the structural changes and the interaction of CV with NaOH. The IR spectra of the as-received and treated samples are displayed in Fig. 2. For reference, the IR spectrum of the solid-phase CV is displayed in Fig. S1(I). The full spectra in the range 500~4000 cm⁻¹ can be seen in Fig. 2(I). In the region of 500~1250 cm⁻¹ shown in Fig. 2(II), multiple peak assignments related to the structure of cellulose can be made. The peaks at 1160, 1054, and 900 cm⁻¹ are attributed to C-O-C asymmetric bridge stretching, C-O stretching vibrations, and β-glycosidic linkages found in cellulose I or C₁H deformation, respectively [33-38]. A strong peak is present in the samples treated with 0.5 M and 1.0 M NaOH at 880 cm⁻¹, which is due to the presence of the alkali [39]. Multiple assignments around 1106 cm⁻¹ have been reported related to the C-O-C glycosidic ether and antisymmetric stretching of the pyranose ring [37, 40].

As shown in Fig. 2(III, 1250~1750 cm⁻¹ wavenumber range),

a small peak at ~1424 cm⁻¹ is present in samples (a) and (b), which becomes broader and increases in intensity in samples (c-e) as NaOH concentration increases. The peak in samples (a) and (b) is assigned to CH₂ symmetric bending of the ring structures in cellulose, while the same peak for samples (c-e) is due to NaOH (Fig. S2(I)) [39, 41]. The peak at 1588 cm⁻¹ is only present in sample (b) and indicates C=C stretching of an aromatic ring vibration in the aromatic nuclei of CV [42]. Please note that the IR spectrum of 0.1 M CV also shows a weak peak at 1588 cm⁻¹, while the peak is not visible in the $1.0\, imes\,10^{-4}$ M CV IR spectrum due to the strong -OH bending mode peak at 1640 cm⁻¹ as shown in Fig. S1(I). To reduce the impact of -OH on the CV peak intensity, a solid phase CV sample was used, and the spectrum clearly reveals that the peak at 1588 cm⁻¹ is due to the CV. As shown in Fig. 2(III), after NaOH treatment, the 1588 cm⁻¹ peak disappeared due to surface coverage by NaOH.

In Fig. 2(IV), all samples displayed peaks at 2851 cm⁻¹ and 2896 cm⁻¹, suggesting -CH stretching, however sample (e) showed a lower intensity compared to samples (a)-(d) [35, 40]. There are peaks of similar intensities at 3275 cm⁻¹ and 3330 cm⁻¹ in all samples that are attributed to the O-H bond in the O(2)H-O(6) and O(3)H-O(5) inter- and intramolecular hydrogen bonds of cellulose [24, 39, 43, 44]. The inset in Fig. 2(IV) shows the absence of a peak that would have implied a transition from cellulose I to II. This result is encouraging because cellulose crystal transformation from I to II may occur at high NaOH concentrations (>3 M) [33, 39]. Based on the FTIR spectra analysis, it can be concluded that the cellulose structure of the cotton fabric was unaffected by both CV and NaOH under the experimental conditions.

As a complementary technique to the FTIR, Raman spectroscopy is also widely used to acquire structural information on organic/inorganic materials. The Raman spectra of the cotton fabric, CV-dyed fabric (control), and NaOH-treated samples are presented in Fig. 3. The cotton fabric spectrum contains strong bands at $\sim\!1098$ cm $^{-1}$ and $\sim\!1122$ cm $^{-1}$ which correspond to the asymmetric and symmetric C-O-C stretching band in a glycosidic linkage, respectively (Fig. 3(I)) [45]. These peaks were also shown on the control and NaOH-treated samples' spectra. In addition to the same peak positions, the intensity ratio of these bands (I $_{1098\text{cm-1}}/I_{1122\text{cm-1}}$) was not changed much, indicating that the molecular structure

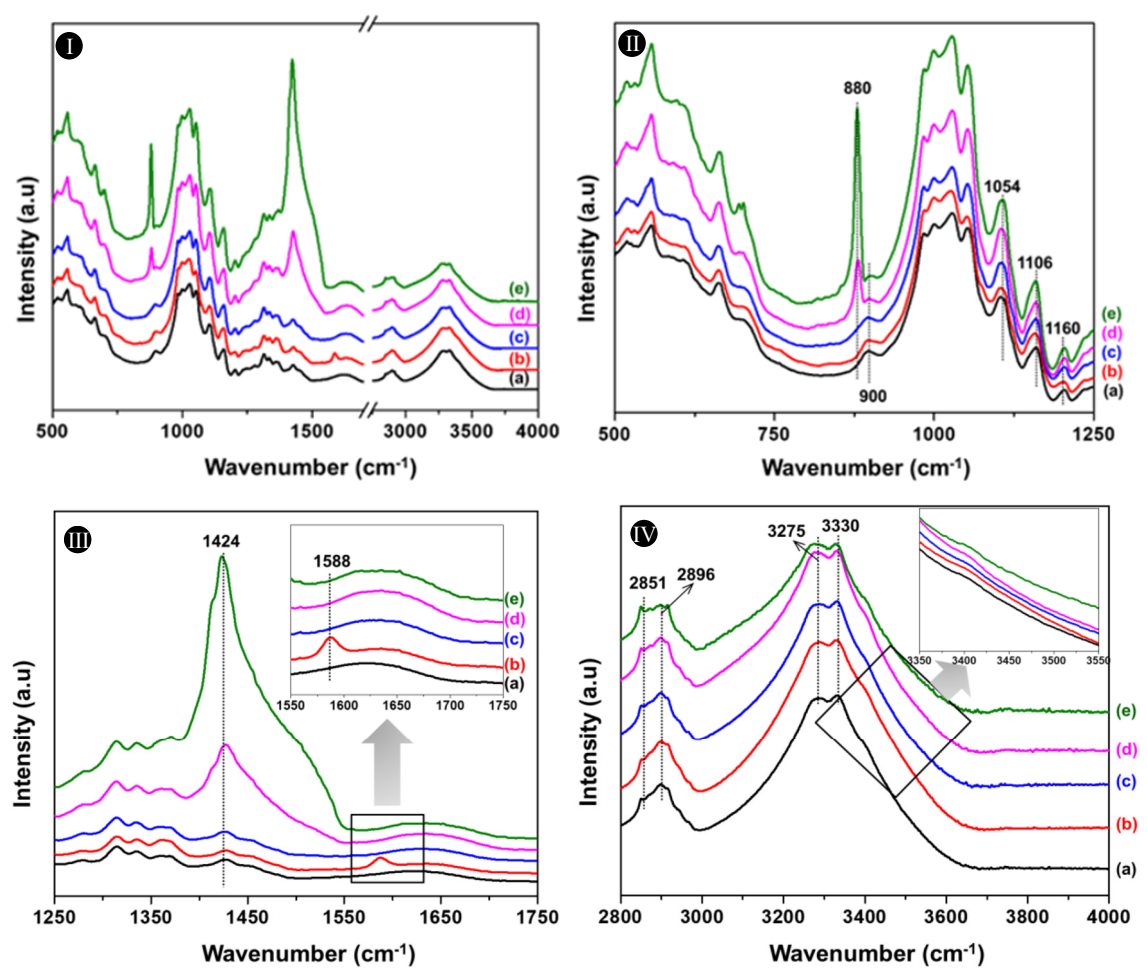


Fig. 2. FTIR spectra of (a) cotton fabric (b) control (cotton fabric+1.0 × 10⁻⁴ M CV) sample (c) control sample treated by 0.1 M NaOH (d) control sample treated by 0.5 M NaOH (e) control sample treated by 1.0 M NaOH; (l) Wavenumber region (cm⁻¹) = 500~4000 cm⁻¹, (II) Wavenumber region (cm⁻¹) = 1250~1750 cm⁻¹, (IV) Wavenumber region (cm⁻¹) = 2800~4000 cm⁻¹. For comparison purposes, the IR spectra were normalized by the CH stretching (2800~3000 cm⁻¹) bands.

of cellulose was not affected by CV dyeing and decolorization processing.

In the case of the control sample's Raman spectrum (Fig. 3(I, b)), unique CV bands are shown in addition to the cotton fabric Raman band. The peak positions are well matched to band positions in the 0.1 M and solid CV Raman spectra as shown in Fig. S1(II): < 450 cm⁻¹ (C⁺-phenyl stretching and C-N-N mode), 900~1400 cm⁻¹ (ring skeletal vibration and C-H in-plane bending mode), 1500~1650 cm⁻¹ (C-H bending and C-C stretching mode in a ring structure) [46-50]. It is worthwhile to note that Raman spectroscopy has advantages over FTIR spectroscopy in identifying the CV species in aqueous solutions due to Raman spectroscopy's insensitivity to water molecules (see the 0.1 M CV peaks in Fig. S1(I) and (II)) [51]. Fig. 3(I-c,d,e) shows Raman spectra for the 0.1, 0.5, and 1.0 M NaOH-treated control samples. The CV-related bands disappear after treatment with NaOH. A similar result was shown in the IR spectra (Fig. 2(III)). Furthermore, the Raman spectra of the NaOH-treated samples are very similar to the cotton fabric spectrum (Fig. 3(I-a)), indicating that most surface CV species disappeared or were covered by NaOH. The Raman spectra in the 2800~3300 cm⁻¹ region (Fig. 3(II)) shows a peak at ~2896 cm⁻¹, which is assigned to a typical C-H bond stretching mode and was not affected by CV and NaOH treatment [45, 52]. Note again that Raman spectroscopy is insensitive to the hydroxyl vibration, while IR spectra contains a broad/strong O-H band at ~3275 cm⁻¹ and ~3330 cm⁻¹ (Fig. 2 (IV)).

It has been reported that using surface-enhanced Raman scattering (SERS) technique with metal nanoparticles, such as gold or silver, could improve the quality of the CV Raman spectrum by decreasing the fluorescent background [53, 54]. It is worthwhile to comment that using a 785 nm laser can possibly avoid the fluorescence issues as shown in Fig. 3(I). Since the presence of CV was visually observed and color parameters indicated dye presence on each sample (Fig. 6 in the *Colorimetric assays* section), it is concluded that Raman spectroscopy has a limitation to detect CV concentrations below 10⁻⁴ M.

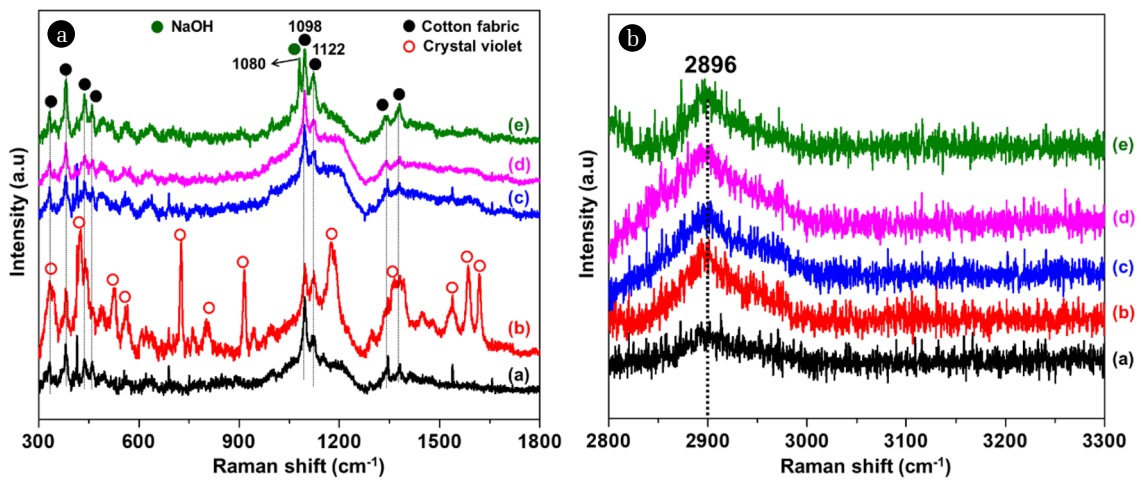


Fig. 3. Raman (785 nm excitation wavelength) spectra of (a) cotton fabric (b) control (cotton fabric+1.0 \times 10⁻⁴ MCV) sample (c) control sample treated by 0.1 M NaOH (d) control sample treated by 0.5 M NaOH (e) control sample treated by 1.0 M NaOH; (I) Raman shift region (Δv) = 300~1800 cm⁻¹, (II) Raman shift region (Δv) = 2800~3300 cm⁻¹. For comparison purposes, the Raman spectra were normalized by the ~1098 cm⁻¹ peak.

3.3. Powder X-ray Diffraction (XRD)

The crystalline structures of the as-received and CV/NaOH-treated samples were investigated using X-ray diffraction (XRD) techniques as shown in Fig. 4. For comparison purposes, all spectra were normalized by an aluminum substrate peak (65°). The characteristic peaks (15.1, 16.9, 22.9, and 34.8°), which are assigned to cellulose I, are observed in all samples. It has been reported that the cellulose I structure can transition to cellulose II, shown by 12° and 20° diffraction patterns, with treatment of high concentrations of NaOH [55]. Because the cellulose peak positions were not shifted, it could be concluded that the bulk

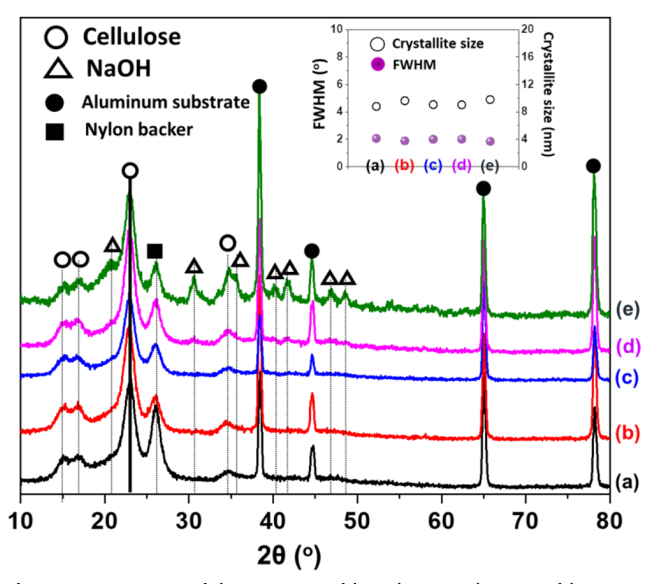


Fig. 4. XRD patterns of the (a) cotton fabric (b) control (cotton fabric+1.0 $\times~10^{-4}$ M CV) sample (c) sample treated by 0.1 M NaOH (d) sample treated by 0.5 M NaOH (e) sample treated by 1.0 M NaOH. Inset: FWHM and crystallite size of cellulose.

material had not lost significant crystallinity during the treatment process. In the case of the 0.5 M and 1.0 M NaOH-treated samples, NaOH characteristic peaks are observed at 30.7, 35.6, 40.2, 41.9, 47.0, and 48.6°, and peak intensity of cellulose was not affected by NaOH treatment. To support that the cellulose structure was unaffected by CV/NaOH treatment, the crystallite size of cellulose was calculated using the Scherrer equation, $D=0.9\lambda/(B\cos\theta)$, where λ is the wavelength (1.54184 Å) of the X-ray used in the experiment, B is the full width at half maximum (FWHM) of the cellulose I peak (22.9°), and θ is the Bragg's angle of the cellulose I peak (22.9°). As shown in Fig. 4 (inset), the FWHM and crystallize size of cellulose were constant, confirming the consistency of the cellulose crystalline structure.

3.4. Scanning Electron Microscopy (SEM) and Energy Dispersive X-ray Spectroscopy (EDS)

To characterize possible changes in fiber morphology and chemistry due to treatment, SEM images were collected in addition to EDS analysis. Fig. 5 shows low resolution images (a~d), high resolution images (a'~d'), and EDS results (a"~d") of the cotton fabric, CV-dyed, and NaOH-treated samples. The mesh dimensions of the cotton fabric were $\sim 300 \ \mu m \times 300 \ \mu m$ and the fabric strands show a flat and smooth surface (Fig. 5(a')). As expected, carbon (C) and oxygen (O) were dominant chemical components, both observed at ~0.25 and ~0.5 keV, respectively (Fig. 5(a")). It was also noticed that the cotton fabric contained trace amounts of an impurity, potassium (K), as a weak peak of K shows at ~3.2 keV. Compared to the cotton fabric, the CV-dyed sample (Fig. 5(b')) shows no distinct differences on neither the fabric surface nor in the chemical composition (Fig. 5(b")), except for the disappearance of the K peak, indicating that the impurity was removed during the dying process. Although the mesh of the cotton fabric was not changed, the strand surfaces were all covered by CV. In the case of NaOH-treated samples, no significant changes (i.e.,

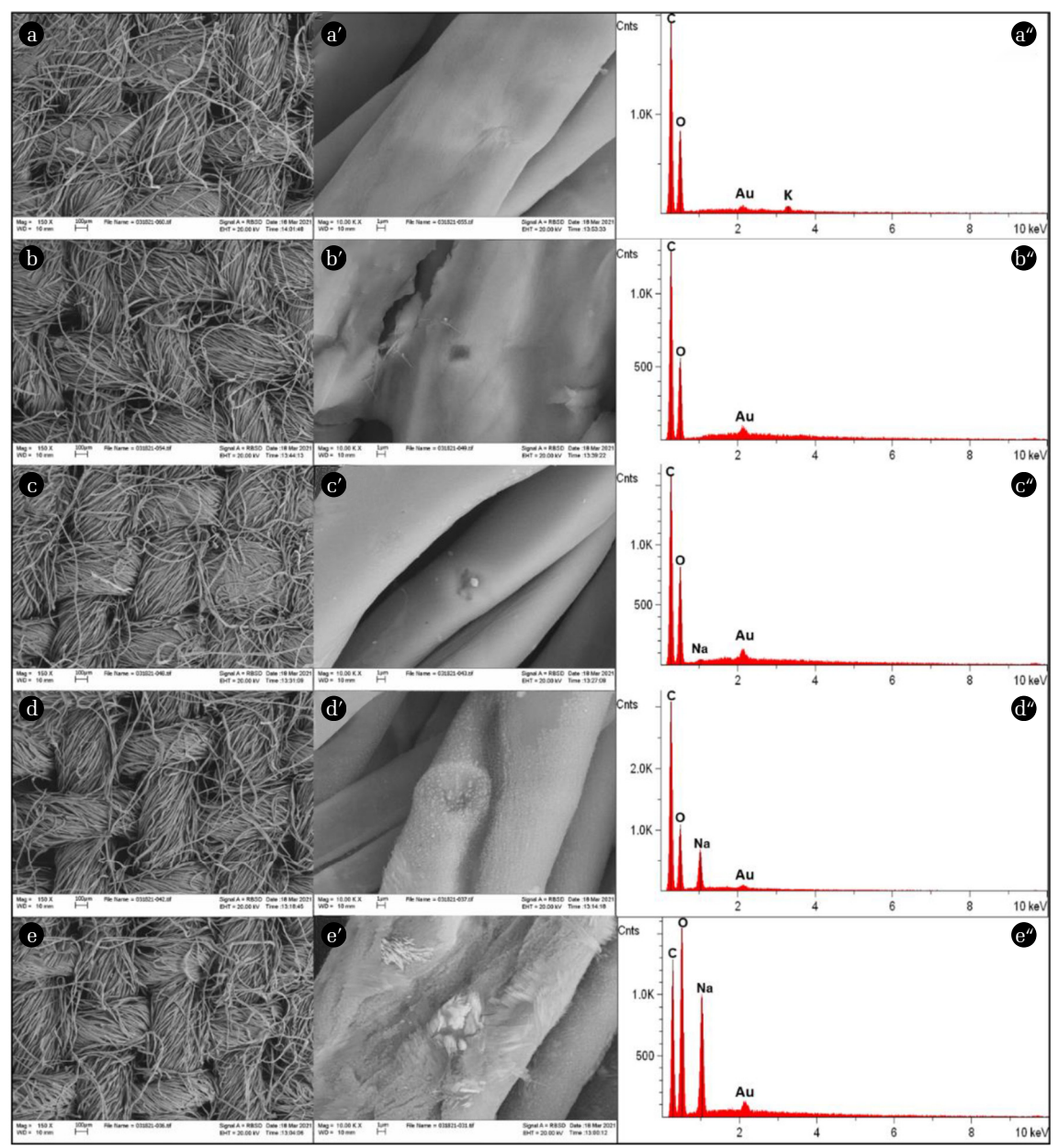


Fig. 5. SEM images and the corresponding EDS results of the (a, a', a") cotton fabric, (b, b', b") control sample (cotton fabric+1.0 × 10⁻⁴ M CV), (c, c', c") control sample treated by 0.1 M NaOH, (d, d', d") control sample treated by 0.5 M NaOH, (e, e', e") control sample treated by 1.0 M NaOH.

mesh dimension and deweaving) on fabric surfaces were noted (Fig. 5 (c-e)). However, it should be highlighted that surface CV had disappeared after interacting with 0.1 M NaOH (Fig. 5 (c')), and that the strand's surface became smooth and round. Furthermore, the EDS result provides the presence of sodium (Na), which is shown at ~1.1 keV (Fig. 5 (c")). Because of the increasing NaOH concentration, the Na peak intensity also increased, and the presence of absorbed Na-containing deposits on strands were clear. Although the presence of NaOH is proved through FTIR (Fig. 2), Raman (Fig. 3), and XRD (Fig. 4), EDS shows the highest

sensitivity for NaOH detecting: EDS (0.1 M NaOH) > FTIR and XRD (0.5 M NaOH) > Raman (1.0 M NaOH). Please note that Raman spectroscopy remained as the most sensitive technique for detecting CV. From the spectroscopic and microscopic results, it is concluded that the crystalline structure of cellulose (or cellulose I) was not affected by CV and NaOH, though the chemical compositions on the strands' surfaces were varied.

3.5. Colorimetric Assays

In conjunction with vibrational spectroscopic analyses, which

provided insight into functional groups present in the samples, a colorimeter was used to measure CIELAB coordinates. Data provided by FTIR and Raman spectroscopies showed that peaks associated with the presence of CV were not detected. Contrary to this data, a violet hue remained on all samples after treatment, indicating the presence of CV. The lack of detection of CV in the treated samples could be explained by a detection limit of both FTIR and Raman spectrometers. This would prevent detection of the reaction products and low CV concentrations, such as that remaining on the fabric. CIELAB coordinates are valuable for characterizing visible changes that may not be distinguishable using the aforementioned methods [56, 57]. These parameters were measured to compare the colorimetry data of CV-dyed and NaOH-treated samples to the fabric as-received (Table 1).

Optical images and the relationship between the L*, a*, and b* values of each sample are displayed in Fig. 6. It is expected that for the sample to be fully decolorized, all values must match those of the fabric as-received. All three parameters for comparing samples must be identical to conclude that they have an identical hue. As the concentration of NaOH was increased, the L* (brightness), a* (red-green coordinate), and b* (yellow-blue coordinate) values

Table 1. CIELAB Coordinates of Cotton Fabric, Control (cotton fabric+1.0 × 10⁻⁴ M CV), and NaOH-Treated Samples. (L* corresponds to brightness (100 = white, 0 = black), a* to the red-green coordinate (positive sign = red, negative sign = green), and b* to the yellow-blue coordinate (positive sign = yellow, negative sign = blue))

Samples	CIELAB values			
	L*	a*	b*	$\Delta \textit{E}_{ab}^{*}$
Cotton fabric	84.88	2.26	12.16	0
Control	38.16	23.19	-38.48	72.01
Control + 0.1 M NaOH	60.16	4.46	-18.17	39.19
Control + 0.5 M NaOH	68.4	2.87	-11.1	28.51
Control + 1.0 M NaOH	73.48	2.6	-3.74	19.57

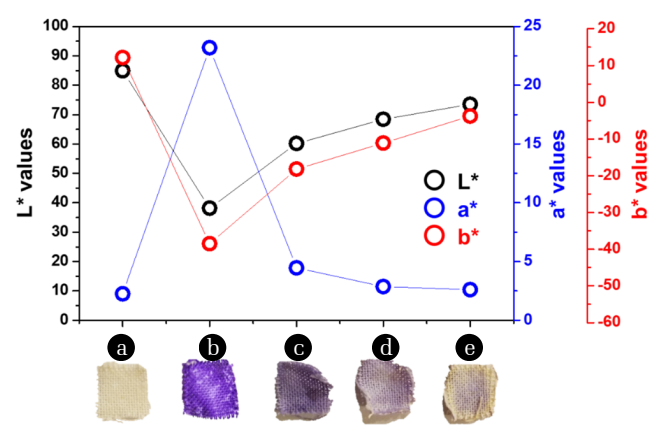


Fig. 6. CIELAB (L*, a*, and b*) values of (a) cotton fabric (b) control (cotton fabric+1.0 \times 10⁻⁴ M CV) sample (c) control sample treated by 0.1 M NaOH (d) control sample treated by 0.5 M NaOH (e) control sample treated by 1.0 M NaOH.

shifted towards those of the cotton fabric sample. For instance, it was observed that CV-dyed fabric treated with a higher NaOH concentration had a greater L* shift from the control sample L* value (38.16) to the cotton fabric L* value (84.88). Comparably, since the b* values are negative for the samples dyed with CV, this represents that yellow radiation was absorbed, indicating that these samples appear more blue than yellow [58]. ΔE_{ab}^* represents the distance between two color points in the CIELAB space [59]. These values were calculated using the formula $\Delta E_{ab}^* = \sqrt{(L_2^* - L_1^*)^2 + (a_2^* - a_1^*)^2 + (b_2^* - b_1^*)^2}$, with L*, a*, and b* from Table 1. The values decreased as the concentration of NaOH was increased, demonstrating that the violet color faded. However, since the lowest value (19.57) is not 0, it is evident that CV remained on the fabric.

3.6. Mechanical Properties

To investigate the influence of the treatment on mechanical properties of the woven cotton muslin samples, tensile testing was conducted on as-received and CV/NaOH-treated cotton fibers. The stress transfer at the fiber interface can be observed by the stress-strain curve as shown in Fig. 7(A). When the load reached the ultimate tensile strength, the dropping of the stress-strain curve differed among the samples. The control and 0.1 M NaOH-treated samples show a moderate slope, indicating that the entangled fiber matrix did not break at the same time. Inversely, the slope of the stress-strain curve of the remaining samples showed is steep, suggesting that the fiber matrix broke immediately.

The calculated ultimate tensile strength is shown in Fig. 7(B). The tensile strength of the samples is similar to the work done by Herrera-Franco and Valadez-González [60]. The Young's modulus and elongation at break of the samples are shown in Fig. 7(C-D). Evidently, the Young's modulus of the treated samples increased with increasing NaOH concentration. Consistently, the samples treated with higher NaOH concentration showed lower elongation at break, indicating lower fracture toughness.

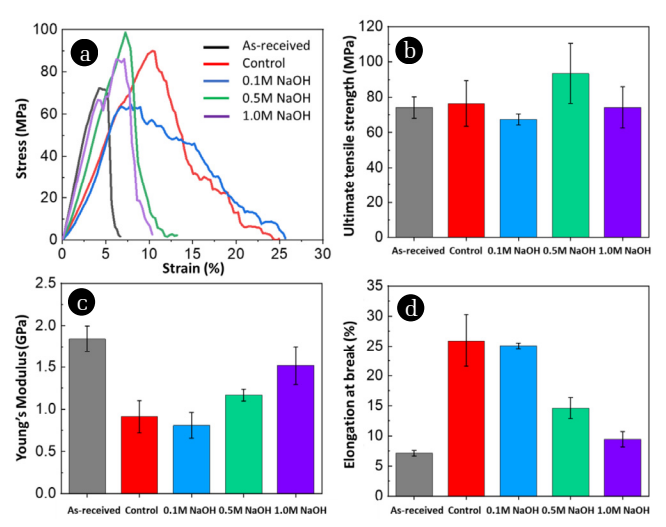


Fig. 7. Mechanical testing analysis of (A) stress strain curve, (B) ultimate tensile strength, (C) Young's modulus, and (D) Elongation at break.

4. Conclusions

Hypothesizing that increasing the concentration of NaOH affects the extent to which CV-stained cotton fabric is decolorized, this article compared NaOH-treated samples against a control sample and the fabric as-received. Results from FTIR and Raman data suggested that all NaOH-treated samples successfully converted CV to the product, while colorimetry data indicated that a violet hue remained in all samples. XRD showed insignificant loss of crystallinity in each sample. SEM images were taken to study the surface morphology of the fabric after being decolorized, with results showing no unweaving of individual strands. The colorimetry results found that as increased concentrations of NaOH were applied, L*, a*, and b* values more closely resembled those of the as-received cotton fabric sample. When comparing the value of CV-dyed fabric treated with 1.0 M NaOH to the fabric as-received, the value did not return to zero, indicating that CV remained on the surface. Additionally, the structural integrity of the fabric did not diminish with increasing NaOH, suggesting the stability of cotton fabric under the testing conditions (0.1 M NaOH~ 1.0 M NaOH). Samples showed increased Young's modulus with increasing concentrations of NaOH. Those treated with lower concentrations of NaOH showed higher elongation at the breaking point, suggesting fracture toughness decreases when cellulose fabric is treated with higher concentrations of NaOH.

As seen from the spectrometer and colorimeter data, as well as the images of the fabric samples, it is evident that there was both a cellulose-CV and CV-NaOH interaction. An improvement could be made to increase the dye removal rate of crystal violet (as well as other synthetic dyes). In this study the authors ran the tests in the static condition only to convert CV to the product as a function of NaOH at room temperature. A mixing method should be considered to accelerate the rate of the reaction, in addition to studying temperature effects. Furthermore, future work will consider *in-situ* characterization methods to verify chemical reaction mechanisms, particularly those related to solid-liquid phase interactions.

Acknowledgements

The authors acknowledge funding support from the National Science Foundation (NSF-CBET-1948422). This work was supported by the Ministry of Education of the Republic of Korea and the National Research Foundation of Korea (NRF 2019S1A5 A2A03054508). The authors would like to thank Prof. Rina Tannenbaum for providing us with the Raman and FTIR spectrometers.

Authors contributions

K.M. (student), M.F. (student), R.H. (student) and T.K. (professor) performed the activity test and characterization experiments, analyzed data, and wrote the draft. Y.L. (student) and M.R. (professor) performed the mechanical testing experiments, analyzed data, and

wrote the draft. G.H (professor), H.J. (professor) and T.K. (professor) initiated the research topic and conceptualization, revised draft, and approved the final manuscript.

Competing interests

The authors declare that they have no conflict of interest.

References

- Shirvanimoghaddam K, Motamed B, Ramakrishna S, Naebe M. Death by waste: Fashion and textile circular economy case. Sci Total Environ. 2020;718:137317. https://doi.org/10.1016/j.scitotenv.2020.137317.
- Degenstein L, McQueen R, McNeill L, Hamlin R, Wakes S, Dunn L. Impact of physical condition on disposal and end-of-life extension of clothing. Int J Consum Stud. 2020;44:586-596. https://doi.org/10.1111/ijcs.12590.
- Environmental Protection Agency. Textiles: Material-specific data, www.epa.gov/facts-and-figures-about-materials-waste-and-recycling/ textiles- material-specific-data.
- Ellen MacArthur Foundation. A new textiles economy: Redesigning fashion's future. Report, Cowes, UK, 2017. https://ellenmacarthurfoundation.org/a-new-textiles-economy
- Johnson S, Echeverria D, Venditti R, Jameel H, Yao Y. Supply chain of waste cotton recycling and reuse: A review. AATCC J. Res. 2020;7:19-31. https://doi:10.14504/ajr.7.S1.3.
- 6. Wedin H, Niit E, Mansoor Z, Kristinsdottir AR, de la Motte H, Jönsson C, et al. Preparation of viscose fibres stripped of reactive dyes and wrinkle-free crosslinked cotton textile finish. J Polym Environ. 2018;26:3603-3612. https://doi.org/10.1007/s10924-018-1239-y.
- Hairif T, Montazer M. A review on textile sonoprocessing: A special focus on sonosynthesis of nanomaterials on textile substrates. Ultrason Sonochem. 2015;23:1-10. https://doi.org/10. 1016/j.ultsonch.2014.08.022.
- Buntić A, Pavolović M, Anotonović D, Šiler-Marinković S, Dimitrijević-Branković S. A treatment of wastewater containing basic dyes by the use of new strain Streptomyces microflavus CKS6. J. Clean. Prod. 2017;148:347-354. https://doi.org/10. 1016/j.jclepro.2017.01.164.
- Javaid R, Qazi U. Catalytic Oxidation Process for the Degradation of Synthetic Dyes; An Overview. Int. J. Environ. Res. 2019; 17:2066-2093. https://doi: 10.3390/ijerph16112066.
- Fatima M, Farooq R, Lindström R, Saeed M. A review on biocatalytic decomposition of azo dyes and electrons recovery.
 J. Mol. Liq. 2017;246:275-281. https://doi.org/10.1016/j. molliq.2017.09.063.
- Robinson T, McMullan G, Marchant R, Nigam P. Remediation of dyes in textile effluent: a critical review on current treatment technologies with a proposed alternative. Bioresour. Technol. 2001;77:247-255. https://doi.org/10.1016/S0960-8524(00)00080-8.
- García-Montaño J, Ruiz N, Muñoz I, Domènech X, García-Hortal JA, Torrades F, et al. Environmental assessment of different photo-Fenton approaches for commercial reactive dye removal.

- J. Hazard. Mater. 2006;138:217-225. https://doi:10.1016/j.jhazmat.2006.05.061.
- Mansfield S, Mooney C, Saddler J. Substrate and enzyme characteristics that limit cellulose hydrolysis. Biotechnol. Prog. 1999;15:804-816. https://doi:10.1021/bp9900864.
- Kamid K, Okajim K, Kowsaka K. Dissolution of natural cellulose into aqueous alkali solution: Role of super-molecular structure of cellulose. Polym. J. 1992;24:71-86. https://doi.org/10.1295/ polymj.24.71.
- Cai J, Zhang L. Rapid dissolution of cellulose in LiOH/urea and NaOH/urea aqueous solutions. Macromol. Biosci. 2005;5: 539-548. https://doi:10.1002/mabi.200400222.
- Duchemin B. Mercerization of cellulose in aqueous NaOH at low concentrations. Green Chem. 2015;17:3941-3947. https:// doi:10.3390/molecules25245834.
- Ozturk H, Bechtold T. Effect of NaOH treatment on the interfibrillar swelling and dyeing properties of lyocell (TENCEL) fibres. Fibres Text. East. Eur. 2007;15:114-117.
- Zhou J, Zhang L. Solubility of cellulose in NaOH/urea aqueous solution. Polym. J. 2000;32:866-870. http://fibtex.lodz.pl/article256.html.
- Chen X, Burger C, Fang D, Ruan D, Zhang L, Hsiao B, et al. X-ray studies of regenerated cellulose fibers wet spin from cotton linter pulp in NaOH/thiourea aqueous solutions. Polym. J. 2006;47:2839-2848. https://doi:10.1016/J.POLYMER.2006.02.044.
- Qi H, Chang C, Zhang L. Effects of temperature and molecular weight on dissolution of cellulose in NaOH/urea aqueous solution. Cellulose. 2008;15:779-787. https://doi.org/10.1007/ s10570-008-9230-8.
- 21. Qi H, Yang Q, Zhang L, Liebert T, Heinze T. The dissolution of cellulose in NaOH-based aqueous system by two-step process. Cellulose. 2011;18:247-245. https://doi:10.1007/s10570-010-9477-8.
- 22. Jin H, Zha C, Gu L. Direct dissolution of cellulose in NaOH/thiourea/urea aqueous solution. Carbohydr. Res. 2007;342:851-858. https://doi.org/10.1016/j.carres.2006.12.023.
- 23. Le Moigne N, Navard P. Dissolution mechanisms of wood cellulose fibres in NaOH–water. Cellulose. 2010;17:31-45. https://doi: 10.1007/s10570-009-9370-5.
- Pei L, Wu J, Wang Q, Wang J. Study of crystal violet hueing dye deposition on fabrics during home laundry. J. Surfactants Deterg. 2016;19:795-801. https://doi.org/10.1007/s11743-016-1831-x.
- Maley M, Arbiser J. Gentian violet: A 19th century drug re-emerges in the 21st century. Exp. Dermatol. 2013;22:775-780. https://doi:10.1111/exd.12257.
- Wakelyn PJ. 14 Health and safety issues in cotton production and processing. In: Gordon S, Hsieh YL, eds. Cotton: science and technology. Cambridge, England: Woodhead Publishing; 2007. p. 460-483. https://doi:10.1533/9781845692483.3.460.
- 27. Du Z, Mao S, Chen Z, Shen W. Kinetics of the reaction of crystal violet with hydroxide ion in the critical solution of 2-butoxyethanol + water. J. Phys. Chem. A. 2013;117:283-290. https://doi.org/10.1021/jp3111502.
- 28. Silva LS, Carvalho J, Bezerra RDS, Silva MS, Ferreira FJL, Osajima JA, et al. Potential of cellulose functionalized with carboxylic acid as biosorbent for the removal of cationic dyes in aqueous solution. Molecules. 2018;23:743. https://doi:10.

- 3390/molecules23040743.
- Corsaro G. Colorimetric chemical kinetics experiment. J. Chem. Educ. 1964;41:48-50. https://doi.org/10.1021/ed041p48.
- Kazmierczak N, Vander Griend A. Improving student results in the crystal violet chemical kinetics experiment. J. Chem. Educ. 2017;94:61-66. https://doi.org/10.1021/acs.jchemed.6b00408.
- 31. Omer A, Elgarhy G, El-Subruiti G, Khalifa R, Eltaweil A. Fabrication of novel iminodiacetic acid-functionalized carboxymethyl cellulose microbeads for efficient removal of cationic crystal violet dye from aqueous solutions. Int. J. Biol. Macromol. 2020; 148: 1072-1083. https://doi:10.1016/j.ijbiomac.2020.01. 182.
- 32. Zaidi N, Lim L, Usman A. Artocarpus odoratissimus leaf-based cellulose as adsorbent for removal of methyl violet and crystal violet dyes from aqueous solution. Cellulose. 2018; 25: 3037-3049. https://doi:10.1007/s10570-018-1762-y.
- Yue Y, Han G, Wu Q. Transitional properties of cotton fibres from cellulose I to cellulose II structure. Bioresources 2013; 8:6460-6471. https://doi:10.15376/BIORES.8.4.6460-6471.
- 34. Zhou Y, Zhang M, Wang X, Huang Q, Min Y, Ma T, et al. Removal of crystal violet by a novel cellulose-based absorbent: comparison with native cellulose. Ind. Eng. Chem Res. 2014;53:5498-5506. https://doi.org/10.1021/ie404135y.
- Carrillo F, Colom X, Suñol J, Saurina J. Structural FTIR analysis and thermal characterisation of lyocell and viscose-type fibres. Eur. Polym J. 2004;40:2229-2234. https://doi.org/10.1016/j. eurpolymj.2004.05.003.
- Kunusa W, Isa I, Laliyo L, Iyabu H. FTIR, XRD and SEM analysis of microcrystalline cellulose (MCC) fibers from corncorbs in alkaline treatment. J. Phys. Conf. Ser. 2018;1028:012199. https://doi:10.1088/1742-6596/1028/1/012199.
- 37. Wang H, Li S, Wu T, Wang X, Cheng X, Li D. A comparative study on the characterization of nanofibers with cellulose I, I/II, and II polymorphs from wood. Polymers. 2019;11:153. https://doi: 10.3390/polym11010153.
- Xing L, Gu J, Zhang W, Tu D, Hu C. Cellulose I and II nanocrystals produced by sulfuric acid hydrolysis of Tetra pak cellulose I. Carbohydr. Polym. 2018;192:184-192. https://doi:10.1016/j. carbpol.2018.03.042.
- Fengel D, Strobel C. FTIR spectroscopic studies on the heterogeneous transformation of cellulose I into cellulose II. Acta Polym. 1994;45:319-324. https://doi:10.1002/actp.1994.010450406.
- Garside P, Wyeth P. Identification of cellulosic fibres by FTIR spectroscopy- thread and single fibre analysis by attenuated total reflectance. Stud. Conserv. 2003;48:269-275. https://doi:10. 2307/1506916.
- 41. Xing L, Hu C, Zhang W, Guan L, Gu J. Biodegradable cellulose I (II) nanofibrils/poly (vinyl alcohol) composite films with high mechanical properties, improved thermal stability and excellent transparency. Int. J. Biol. Macromol. 2020;164:1766-1775. https://doi.org/10.1016/j.ijbiomac.2020.07.320.
- 42. Marco-Brown JL, Guz L, Olivelli MS, Schampera B, Torres Sánchez RM, Curutchet G, et al. New insights on crystal violet dye adsorption on montmorillonite: Kinetics and surface complexes studies. Chem. Eng. J. 2018;333:495-504. https://doi.org/10.1016/j.cej.2017.09.172.
- 43. Fabryanty R, Valencia C, Soetaredjo FE, Putro JN, Santoso SP,

- Kurniawan A, et al. Removal of crystal violet dye by adsorption using bentonite alginate composite. J Environ. Chem. Eng. 2017;5:5677-5687. https://doi.org/10.1016/j.jece.2017.10.057.
- 44. Sun P, Hui C, Wang S, Wan L, Zhang X, Zhao Y. Bacillus amyloliquefaciens biofilm as a novel biosorbent for the removal of crystal violet from solution. Colloids Surf. B. 2016; 139:164-170. https://doi:10.1016/j.colsurfb.2015.12.014.
- 45. Edwards HGM, Farwell DW, Williams AC. FT-Raman spectrum of cotton: a polymeric biomolecular analysis. Spectrochim. Acta A Mol. Biomol. Spectrosc. 1994;50A:807-811. https://doi.org/10.1016/0584-8539(94)80016-2.
- 46. Sanci R, Volkan M. Surface-enhanced Raman scattering (SERS) studies on silver nanorod substrates. Sens. Actuators B Chem. 2009;139:150-155. https://doi:10.1016/j.snb.2008.10.033.
- Zhang DH, Liu XH, Wang X. Synthesis of single-crystal silver slices with predominant (1 1 1) facet and their SERS effect. J. Mol. Struct. 2011;985:82-85. https://doi:10.1016/j.molstruc. 2010.10.024.
- 48. Liang EJ, Ye XL, Kiefer W. Surface-enhanced Raman spectroscopy of crystal violet in the presence of halide and halate ions with near-infrared wavelength excitation. J. Phys. Chem. A. 1997;101:7330-7335. https://doi.org/10.1021/jp971960j.
- Alyami A, Barton K, Lewis L, Mirabile A, Iacopino D. Identification of dye content in colored BIC ballpoint pen inks by Raman spectroscopy and surface- enhanced Raman scattering. J. Raman Spectrosc. 2019;50:115-126. https://doi.org/10.1002/jrs.5512.
- 50. Saviello D, Trabace M, Alyami A, Mirabile A, Baglioni P, Giorgi R, et al. Raman spectroscopy and surface enhanced Raman scattering (SERS) for the analysis of blue and black writing inks: Identification of dye content and degradation processes. Front. Chem. 2019;7:727-736. https://doi.org/10.3389/fchem. 2019.00727.
- Kim T, Assary R, Curtiss L, Marshall C, Stair P. Vibrational properties of levulinic acid and furan derivatives: Raman spectroscopy and theoretical calculations. J. Raman Spectrosc. 2011;42:1069-2076. https://doi.org/10.1002/jrs.2951.

- 52. Kavkler K, Demsar A. Application of FTIR and Raman Spectroscopy to Qualitative Analysis of Structural Changes in Cellulosic Fibres. Tekstilec. 2012;55:19-31. http://www.tekstilec. si/wp-content/uploads/2012/01/Application-of- FTIR-and-Raman-Spectroscopy-to-Quantitative-Analysis-os-Structural-Changes-in-Cellulosic-Fibres.pdf.
- 53. Mao A, Jin X, Gu X, Wei X, Yang G. Rapid, green synthesis and surface-enhanced Raman scattering effect of single-crystal silver nanocubes. J. Mol. Struct. 2012;1021:158-161. https://doi.org/10.1016/j.molstruc.2012.04.043.
- 54. Fateixa S, Nogueira HIS, Trindade T. Surface-enhanced Raman scattering spectral imaging for the attomolar range detection of crystal violet in contaminated water. ACS Omega 2018;3:4331-4341. https://doi.org/10.1021/acsomega.7b01983.
- Liu Y, Hu H. X-ray diffraction study of bamboo fibers treated with NaOH. Fibers Polym. 2008;9:735-739. https://doi.org/ 10.1007/s12221-008-0115-0.
- 56. Fiedler JO, Carmona ÓG, Carmona CG, Lis MJ, Plath AMS, Samulewski RB, et al. Application of Aloe vera microcapsules in cotton nonwovens to obtain biofunctional textiles. J. Text. Inst. 2019;111:68-74. https://doi.org/10.1080/00405000.2019. 1625607.
- Papancea A, Patachia S, Dobritoiu R. Crystal violet dye sorption and transport in/through biobased PVA cryogel membranes.
 J. Appl. Polym. Sci. 2015;132:41838. https://doi:10.1002/app.41838.
- Papancea A, Patachia S. Characterization of dyes loaded polyvinyl alcohol (PVA) based hydrogels through CIELAB method. Environ Eng Manag J. 2015;14:361-371. https://doi:10.30638/ eemj.2015.037.
- McGrath J, Beck M, Hill M. Replicating Red: Analysis of ceramic slip color with CIELAB color data. J. Archaeol. Sci. Rep. 2017;14:432-438. https://doi.org/10.1016/j.jasrep.2017.06.020.
- Herrera-Franco P, Valadez-González A. A study of the mechanical properties of short natural-fiber reinforced composites. Compos. B. Eng. 2005;36:597-608. https://doi.org/10.1016/j.compositesb.2005.04.001.